



**QUEEN'S
UNIVERSITY
BELFAST**

Novel volumetric imaging biomarkers for assessing disease activity in eyes with PCV

Vyas, C. H., Cheung, C. M. G., Jordan-Yu, J. M. N., Shimizu, H., Tan, A. C. S., Sim, S. S., Fenner, B. J., Akiba, M., Chakravarthy, U., & Teo, K. Y. C. (2022). Novel volumetric imaging biomarkers for assessing disease activity in eyes with PCV. *Scientific Reports*, 12, Article 2993. <https://doi.org/10.1038/s41598-022-06742-2>

Published in:
Scientific Reports

Document Version:
Publisher's PDF, also known as Version of record

Queen's University Belfast - Research Portal:
[Link to publication record in Queen's University Belfast Research Portal](#)

Publisher rights

Copyright 2022 the authors.

This is an open access article published under a Creative Commons Attribution License (<https://creativecommons.org/licenses/by/4.0/>), which permits unrestricted use, distribution and reproduction in any medium, provided the author and source are cited.

General rights

Copyright for the publications made accessible via the Queen's University Belfast Research Portal is retained by the author(s) and / or other copyright owners and it is a condition of accessing these publications that users recognise and abide by the legal requirements associated with these rights.

Take down policy

The Research Portal is Queen's institutional repository that provides access to Queen's research output. Every effort has been made to ensure that content in the Research Portal does not infringe any person's rights, or applicable UK laws. If you discover content in the Research Portal that you believe breaches copyright or violates any law, please contact openaccess@qub.ac.uk.

Open Access

This research has been made openly available by Queen's academics and its Open Research team. We would love to hear how access to this research benefits you. – Share your feedback with us: <http://go.qub.ac.uk/oa-feedback>



OPEN

Novel volumetric imaging biomarkers for assessing disease activity in eyes with PCV

Chinmayi Himansuroy Vyas¹, Chui Ming Gemmy Cheung^{1,2}, Janice Marie N. Jordan-Yu¹, Hitoshi Shimizu³, Anna Cheng Sim Tan^{1,2}, Shaun Sebastian Sim¹, Beau James Fenner¹, Masahiro Akiba³, Usha Chakravarthy⁴ & Kelvin Yi Chong Teo^{1,2}✉

The aim of this study was to evaluate influence of baseline imaging features on visual and anatomical outcomes in eyes with PCV treated with anti-VEGF monotherapy. In this prospective study we enrolled participants with treatment-naïve PCV who followed a treat-and-extend protocol using intravitreal aflibercept (IVA) monotherapy. Baseline clinical features evaluated included best corrected visual acuity (BCVA), traditional features such as lesion size, fluid-related OCT parameters and novel parameters using automated software. This included quantitative and qualitative pigment epithelium detachment (PED) parameters [height, volume]; and choroidal parameters. [choroidal thickness (CT), choroidal volume (CV) and choroidal vascularity index (CVI)]. We evaluated the predictive value of each parameter on visual and anatomical outcome at month 12. We additionally evaluated initial treatment response after 3 monthly injections with respect to month 12 outcomes. Fifty-two eyes from 52 participants were included in the study. The BCVA increased from 61.1 ± 13.2 to 69.6 ± 13.2 early treatment diabetic retinopathy study (ETDRS) letters ($p < 0.01$) and CRT reduced from $455.7 \pm 182.4 \mu\text{m}$ to 272.7 ± 86.2 ($p < 0.01$) from baseline to month 12. The proportion of eyes with PED decreased significant from 100% at baseline to 80% at month 12 ($p < 0.01$). Reduction in the mean maximum height of PED (from $381.3 \pm 236.3 \mu\text{m}$ to $206.8 \text{ vs } \pm 146.4 \mu\text{m}$) and PED volume (from $1322 \pm 853 \text{ nl}$ to $686 \pm 593 \text{ nl}$) ($p < 0.01$) was also noted from baseline to month 12. Baseline features associated with better month 12 BCVA included baseline BCVA ($\beta = -0.98$, 95%CI -3.38 to -1.61 , $p = 0.02$) and baseline CRT ($\beta = -0.98$, 95%CI -1.56 to -0.40 , $p = 0.04$) while the disease activity at month 12 was significantly associated with lower baseline CRT (366.0 ± 129.5 vs 612.0 ± 188.0 , $p < 0.001$), lower baseline PED height (242.0 ± 150.0 vs $542.0 \pm 298.0 \mu\text{m}$, $p < 0.01$), lower baseline PED volume ($0.6 \pm 0.3 \text{ mm}^3$ vs $2.2 \pm 1.3 \text{ mm}^3$ vs, $p < 0.01$), lower proportion with marked CVH (17.9% vs 46.2%, $p = 0.02$) and lower mean CVI (61.8 ± 1.4 vs 63.0 ± 1.4 , $p < 0.02$). Additionally, a larger decrease in CRT (per 100 nm) and larger PED volume reduction (per 100 nl) at month 3 from baseline were associated with greater BCVA gain and inactive disease. PED-related volumetric parameters have an additional predictive value to traditional biomarkers of disease activity in eyes with PCV undergoing anti-VEGF monotherapy. With increasingly precise quantification, PEDs can be a crucial biomarker in addition to traditional parameters and may aid in retreatment decisions.

Optical coherence tomography (OCT) has provided valuable information regarding the retinal microstructure to guide treatment and prognosticate outcome in eyes with neovascular AMD treated with anti-vascular endothelial growth factor (VEGF)^{1–3}. In current clinical practice, non-monthly regimens like treat and extend (TAE) and pro re nata (PRN) relies heavily on disease activity detected on OCT and other modalities to dictate the retreatment criteria. These well-recognized imaging biomarkers include the presence of sub/intra retinal fluid on OCT and haemorrhage detected on clinical examination.

Polypoidal choroidal vasculopathy (PCV) is considered a subtype of neovascular age related maculopathy (nAMD) which is characterized by polypoidal lesions at the termini of a type 1 macular neovascularization detected on indocyanine green angiography (ICGA)^{4–8}.

¹Singapore Eye Research Institute, Singapore National Eye Centre, 11 Third Hospital Avenue, Singapore 168751, Singapore. ²Duke-NUS Medical School, National University of Singapore, Singapore, Singapore. ³Topcon, Tokyo, Japan. ⁴Ophthalmology and Vision Sciences, Queen's University, Belfast, UK. ✉email: kelvin.teo.y.c@singhealth.com.sg

Anti VEGF monotherapy for PCV has been popularized in clinical practice^{9,10}. After the favourable visual outcomes demonstrated in clinical trials such as PLANET and ALTAIR^{11,12}. These studies also base retreatment decisions on disease activity assessed by a combination of clinical and OCT-based criteria. Specifically, increase in fluid on OCT was considered evidence of disease activity. However, beyond IRF and SRF, two OCT-based imaging features have been proposed to be particularly relevant in eyes with PCV, but are currently not routinely incorporated into clinical assessment^{13–22}. Firstly, the influence of pigment epithelial detachment (PED), on visual outcome remains poorly understood^{21,23–29}. Secondly, choroidal congestion is also increasingly believed to be key in the pathophysiology and subsequent treatment response but are inconsistently evaluated in prior studies.

Inconsistencies in **results** from previous studies regarding the influence of PED and choroidal congestion may be due to the lack of standardized quantification methods. Most prior studies use rudimentary, suboptimal quantitative measurements of single point measurement of both PED and sub-foveal choroidal thickness^{18,19,30}. These measurements may not capture changes within the larger macula region which a volumetric measurement can. Recent advances in segmentation algorithms coupled with manual correction can help address the shortcomings in the accuracy of PED and choroidal measurements. These algorithms can generate segmentation lines to delineate PED and choroid throughout the macula volume scan, allowing accurate thickness and volumetric measurements of the different retinal layers and the choroid within the central 6 mm of the posterior pole. In addition, there has been increasing interest in evaluating whether choroidal parameters such as choroidal hyperpermeability (CVH), or choroidal vascularity index (CVI) may influence treatment response^{14,31–33}.

We recently reported the results of a randomized clinical trial comparing two regimens of intravitreal aflibercept in eyes with PCV³⁴. The mean BCVA improvement was +7.9 (5.2 to 10.4) letters in the treat-and-extend arm, which was non-inferior to +8.1 (6.5 to 10.6) letters in the fixed dosing arm at one year. Fluid free retina was achieved in similar proportions in the two arms (76% in the treat-and-extend arm; 83% in the fixed dosing arm) at one year. In the current report, we evaluate the influence of “traditional” baseline imaging features such as the presence or absence of fluid in different retina compartments as well as novel, volumetric quantitative PCV specific imaging biomarkers on visual and anatomical outcomes.

Methods

Study design and population. We analysed clinical and imaging data of participants who were enrolled into a randomized controlled trial in PCV (NCT03117634). Detailed methods and primary outcomes have been published. This study was approved by the SingHealth centralized institutional review board and conducted according to the tenets of the declaration of Helsinki. Written informed consent was provided by all participants prior to study enrolment. No experimental animals were used in the study.

Detailed inclusion criteria and exclusion criteria has been described previously³⁴. Briefly, this study compared efficacy of two treatment strategies in eyes with treatment naïve macular-involving PCV. After the initial induction phase with aflibercept monotherapy (week 0,4,8), all eyes were randomized to a treat and extend (T&E) retreatment strategy as defined in the protocol and were followed up prospectively for 12 months. All participants were randomized at week 12 after a repeat ICGA and OCT in to either personalised arms or fixed arms at a 3:1 ratio. Participants in the fixed arm went to receive six doses of 8 weekly aflibercept injections for the remaining duration of the study. In personalised arm participants with a completely regressed polypoidal lesion (PL) on ICGA commenced T&E phase while participant with active PL lesion on ICGA continued 4 weekly aflibercept injections till week 24 and commenced T&E phase thereafter. Retreatments during the T&E phase depended on the protocol specific retreatment criteria.

Study outcomes and assessment. The outcome measures of interest were: (1) Change in Best Corrected Visual Acuity (BCVA) at month 12 from baseline, which was measured in ETDRS letters and (2) The evidence of disease activity [defined using “traditional” biomarkers such as the presence of new hemorrhage and/or fluid in the subretinal (SRF) and/or intra-retinal space (IRF) on SD-OCT at month 12].

Singapore National Eye Centre ocular reading centre (SORC) acted as a centralised reading centre (CRC) for confirmation of the diagnosis of PCV (Everest criteria)³⁵ prior to randomization in the treatment trial and for all image analysis and grading for the purposes of this study. The analysis of all quantitative and qualitative features were performed by two independent trained graders who were masked to treatment and BCVA. Disagreements between graders were resolved through open arbitration with supervising specialists. All patients underwent colour fundus photo (CFP), OCT (SD-OCT and SS-OCT), fundus fluorescein angiography (FFA) and indocyanine green angiography (ICGA). Imaging acquired at baseline, month 3 and month 12 were used in this study.

Image acquisition. The Colour fundus photo (CFP) were acquired on digital mydriatic retinal camera (TRC-50X/IMAGEnet 2000, Topcon, Tokyo, Japan). The SD-OCT raster scans with enhanced depth imaging were acquired on a 30° × 20° (9 × 6 mm) macular region centred on the fovea, in the high speed mode, with 25 B-scans per volume scan. Each B-scan was averaged (ART mode) using 9 frames using spectralis OCT (Heidelberg Engineering, Heidelberg, Germany). A repeat OCT was acquired on a swept source OCT (SS-OCT) platform (Topcon DRI OCT Triton /version 10.17.003.03, Tokyo, Japan). The SS-OCT scans were acquired on a 6 × 6 mm scan centred on the fovea with a 1050 nm wavelength scanning laser to capture 100,000 A scans per second allowing a rapid and greater penetration of vitreous, retina, choroid and sclera compared to SD-OCT. Dye angiography (FFA and ICGA) were acquired by a confocal scanning laser ophthalmoscope (cSLO) (Spectralis OCT, Heidelberg Engineering, Heidelberg, Germany).

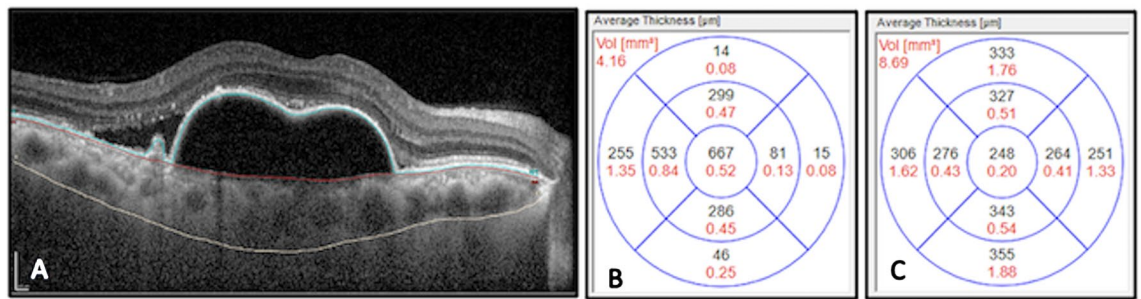


Figure 1. EDI-OCT segmentation of retinal layers and Quantification of PED and choroid thickness and volume. Manual segmentation (A) of retinal layers: outer margin of the Retinal Pigment Epithelium (blue line), inner margin of the Bruch's membrane (red line) and choroid-scleral interface (white line) to generate both volume (mm³) within the central 6 mm OCT ETDRS grid and thickness (µm) maps of (B) PED volume and (C) choroid thickness in treatment naïve eyes with PCV.

Image assessment and grading criteria. Sub-retinal blood was defined as the presence of retinal haemorrhage more than 4 disc diameter in-area on the CFP. Area of the Sub-retinal blood was measured using the inbuilt measuring tool available in IMAGENetR4 digital imaging system. (version 4.2.1, Topcon, Tokyo, japan).

Baseline BNN and PL areas were measured using the free hand drawing tool of the spectralis heidelberg eye explorer (HEYEX) image management platform (version 1.10.4.0) and the region encompassed by the lesion was outlined on selected ICGA frames captured between 5–6 min.

CVH was assessed based on comparison of baseline, mid-phase (5–7 min) and late-phase ICGA (10–15 min) ICGA. We defined CVH as marked if there is presence of patchy hyper fluorescence with blurred margins persisted from the mid to the late phase ICGA, mild if there is fuzziness of choroidal vessels in mid-phase ICGA but no patchy hyper fluorescence in late phase, and absent if none of the above features was present.

All the SD-OCT scans were graded for presence of SRF, IRF and PED. SRF was defined by an area of round or oval hypo-reflectivity with clear borders located within the retinal tissue. IRF was defined as widening of the retinal bands as compared to normal healthy retina. PEDs were defined as focal elevations of the reflective retinal pigment epithelium (RPE) band over an optically clear or moderately reflective space. For this study, a minimum height of 100 µm for PED was used²⁹. Quantitative measures were done using the calliper function on HEYEX image management platform (version 1.10.4.0). The quantitative features measured using this calliper function included central retinal thickness (CRT), PED height and choroidal thickness (CT). Central retinal thickness was obtained by automated measurement of the HEYEX software as the distance between the ILM and the outer RPE boundary at BM at the fovea. Maximum PED height (µm) was measured as the vertical measurement between the outer border of the BM and the inner border of the RPE of the highest PED. The CT was measured manually from the outer margin of the RPE to the CSI in the fovea (central 1 mm).

Volumetric measurements. The PED volume was derived from RPE-BM volume map generated automatically by the HEYEX software and reflected as PED volume within the central 6 mm ETDRS grid. The software automatically segmented the outer margin of the RPE and inner margin of the BM and computed the volume using the 25 line raster OCT scans. The accuracy of all the automated segmentation was checked by graders who manually adjusted in case of inaccurate placement (Fig. 1).

Macular Choroidal volume (CV) was measured based on a volumetric map between the BM and the choroid scleral interface (CSI). The CSI segmentation line was manually placed (JJ) within the central 6 mm zone, the subsequent volume map was generated automatically and CV computed using the 25 line raster OCT scans. All volumetric measurements were generated at baseline, month 3 and month 12.

Choroidal vascular index (CVI). CVI values were generated using structural scans acquired with the swept-source OCTA protocol (Topcon, Japan). Four single B-scan images were captured in same location and were overlapped and further averaging method was applied with consecutive five frames to generate representative B-scan to increase the signal to noise ratio. BM and CSI were automatically delineated with beta segmentation algorithm and manually adjusted by graders if inaccurate. Binarization technique was applied using Niblack method. CVI was expressed as the luminal area/total choroidal area was generated for each B-scan. Volumetric CVI for the 6 × 6 mm scanned area centered over the fovea was calculated as the average CVI of all individual B-scans (Fig. 2).

Impact of the change from baseline to month 3 in OCT determined macular morphology on month 12 outcomes. Baseline morphological parameters were initially assessed and those found to be significant ($p < 0.05$) were further studied at month 3 to understand the association of change in these factors from baseline to treatment outcomes at month 12. Features that were analysed included baseline to month 3 1) Mean change in CRT (per 100µm), 2) Mean change in PED volume (per 100 nl) 3) Mean change in PED height (per 100µm) and 4) Mean change in CV (per 100 nl).

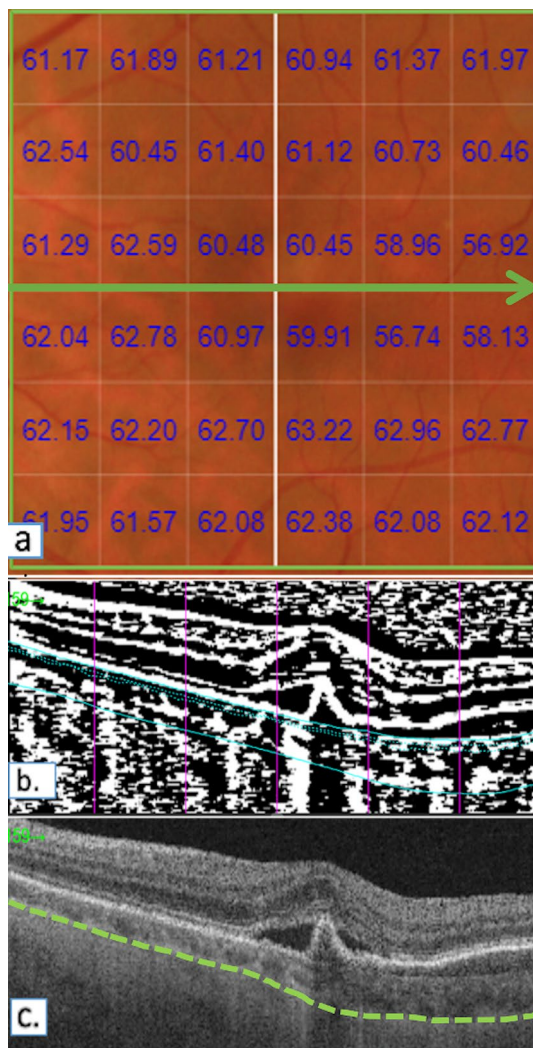


Figure 2. Choroidal vascularity index values generated using structural scans acquired with the swept- source OCTA protocol. (a) Automatically generated volumetric CVI values superimposed over the 6×6 mm macular area. (b) Representative binarized SS-OCT image using Niblack binarization technique at the location of the green arrow. The vertical pink lines indicate the position along the B-scan, in relation to the En-face image. The solid blue lines indicate the inner and outer borders of the choroidal segmentation. i.e. bruch's membrane and choroid-scleral interface respectively. The dotted blue further segments the 'inner choroid'. (c) Original SS-OCT image at the green arrow. The green line represents the manually marked choroid-scleral interface.

Statistical analysis. We summarized continuous data with means and standard deviations (SD), while categorical variables with counts and percentages. Within group changes from baseline to month 12 were assessed using a paired *t*-test and Mc-Nemar's Test for continuous and categorical variables, respectively. Comparisons between groups were evaluated using independent T-tests and Chi-Square Tests, respectively for continuous and categorical data.

The BCVA change and disease activity status at month 12 were defined as the two main response variables. Baseline characteristics like patient factors (age, gender), baseline BCVA, ocular factors (baseline CRT, total lesion area, branching neovascular network (BNN) area, PL area, PED height, PED volume, CT, CV, CVH, CVI) and treatment given (injection number) were analysed against these response variables to establish a correlation. Backward stepwise regression was used to reduce the number of variables and the final model was built on the final variables derived from this stepwise regression. Variables with significance level of $p < 0.05$ were retained for further analysis. Multiple linear regression was used for the final model to describing changes in BCVA and estimated coefficient along with their 95% CI and *p*-values. For the association of disease activity adjusted odds ratios (ORs) with 95% CI and *p*-values were presented for each factor in multiple logistic regression models. A repeat analysis was performed to analyse the relationship between these response variables and month 3 treatment outcomes. Statistical analyses were performed using the Stata statistical software: Release 16 (StataCorp LLC, College Station, TX, USA). Statistical significance was set at less than 0.05.

		Baseline	Month 12	<i>p</i>
Age, years	Mean (SD)	69.2 (8.6)	–	–
Gender, female	n (%)	33 (63.5)	–	–
Best corrected visual acuity, letters	Mean (SD)	61.1 (13.2)	69.6 (14.3)	<0.01
Best corrected visual acuity, letters	Median (IRQ)	64 (53, 72)	73 (61, 80)	<0.01
central retinal thickness, μm	Mean (SD)	455.7 (182.4)	272.7 (86.2)	<0.01
central retinal thickness, μm	Median (IRQ)	398 (336, 548)	252 (227, 306)	<0.01
Presence of SRF	n (%)	49 (94.2)	9 (17.3)	<0.01
Presence of IRF	n (%)	8 (15.4)	6 (11.5)	0.6
Presence PED	n (%)	52 (100.0)	40 (80.0)	<0.01
PED height, μm	Mean (SD)	381.3 (236.3)	206.8 (146.4)	<0.01
PED height, μm	Median (IRQ)	332 (225, 462)	185 (155, 225)	<0.01
PED volume, nl	Mean (SD)	1322 (853)	686 (593)	<0.01
PED volume, nl	Median (IRQ)	785 (530, 1585)	540 (405, 808)	<0.01
Choroidal thickness, μm	Mean (SD)	270.9 (96.4)	257.9 (115.0)	0.53
Choroidal thickness, μm	Median (IRQ)	263 (209, 348)	242 (191, 293)	0.21

Table 1. Comparison of features between baseline and month 12. *SRF* sub-retinal fluid; *IRF* intra-retinal fluid, *PED* pigment epithelium detachment; *p* value calculated using chi-square test, *t* test, Mc-Nemar's Test or Wilcoxon rank sum test.

Results

Fifty-two eyes from 52 participants were included in the study. The mean age of participants was 69.2 ± 8.6 (range: 49–87) years, and 63.5% (33) were male. Comparison of features between baseline and month 12 are summarized in Table 1. From baseline to month 12, the mean BCVA increased from 61.1 ± 13.2 to 69.6 ± 13.2 ETDRS letters ($p < 0.01$) and the mean CRT reduced from $455.7 \pm 182.4 \mu\text{m}$ to $272.7 \pm 86.2 \mu\text{m}$ ($p < 0.01$). The proportion of eyes with SRF reduced significantly from 94.2% (49) to 17.3% (9) ($p < 0.01$), while proportion of eyes with IRF reduced from 15.4% (8) at baseline to 11.5% (6) ($p = 0.6$). The proportion of eyes with PED decreased significantly from 100 to 80%, $p < 0.01$, the mean maximum height of PED reduced significantly from $381.3 \pm 236.3 \mu\text{m}$ to $206.8 \pm 146.4 \mu\text{m}$ ($p < 0.01$) and mean PED volume reduced significantly from $1322 \pm 853 \text{ nl}$ to $686 \pm 593 \text{ nl}$. Choroidal thickness (CT) did not show significant change from baseline to month 12, but choroidal volume (CV) of the whole scan area reduced significantly from $6.7 \pm 2.0 \text{ mm}^3$ to $6.3 \pm 2.4 \text{ mm}^3$ from baseline to month 12 ($p = 0.02$). Similar associations were demonstrated when eyes were stratified according to treatment arms.

Associations of baseline parameters with BCVA change at month 12 from baseline (Table 2). Among the baseline features evaluated, lower baseline BCVA (per letter) ($\beta = -0.19$, 95%CI -0.59 to -0.21 , $p < 0.01$), lower baseline CRT (per 100 μm) ($\beta = -0.82$, 95%CI -1.22 to -0.42), $p = 0.03$) and smaller PED volume ($\beta = -1.02$, 95% CI -1.35 to -0.68 , $p < 0.01$) were significantly associated with better vision at month 12. In the multivariate analysis, baseline BCVA ($\beta = -0.98$, 95%CI -3.38 to -1.61 , $p = 0.02$) and baseline CRT ($\beta = -0.98$, 95%CI -1.56 to -0.40 , $p = 0.04$) remained significantly associated with better vision at month 12. None of the choroidal parameters, including baseline choroidal thickness, choroidal volume, CVH and CVI and change in these had significant associations with BCVA at month 12.

Associations of baseline parameters with disease activity month 12 (Table 3). At month 12, 25% (13 eyes) had active disease. Associations of baseline characteristics with disease activity at month 12 are summarized in Table 3. Compared to eyes with active disease, eyes with inactive disease at month 12 had lower baseline CRT (366.0 ± 129.5 vs 612.0 ± 188.0 , $p < 0.001$), lower baseline PED height ($242.0 \pm 150.0 \mu\text{m}$ vs $542.0 \pm 298.0 \mu\text{m}$, $p < 0.01$), lower baseline PED volume ($0.6 \pm 0.3 \text{ mm}^3$ vs $2.2 \pm 1.3 \text{ mm}^3$ vs, $p < 0.01$), lower proportion with marked CVH (17.9% vs 46.2%, $p = 0.02$) and lower mean CVI (61.8 ± 1.4 vs 63.0 ± 1.4 , $p < 0.02$) (Fig. 3). These changes remained significant in the multivariate model.

Associations of OCT macular morphology change from baseline to M3 with outcomes at month 12 (Table 4). In addition to baseline features, we also evaluated whether OCT morphological changes from baseline to month 3 was associated with visual and anatomical outcome at month 12. In the multivariate analysis, a larger decrease in CRT and a larger reduction in PED volume at month 3 from baseline were associated with greater BCVA gain at month 12 (CRT $\beta = 0.51$ per 100 nm, 95%CI 0.12 to 2.18, $p = 0.03$; PED volume $\beta = 1.04$ per 100 nl, 95%CI 0.07 to 2.01, $p = 0.03$) and with inactive disease at month 12 (CRT $\beta = 1.32$ per 100 nm, 95% CI 1.03 to 2.82, $p = 0.03$; PED volume $\beta = 1.39$ per 100 nl, 95%CI 1.11 to 1.82, $p = 0.01$).

Feature	Univariate analysis	<i>p</i>	Multivariate analysis	<i>p</i>
Age	0.32 (−0.13 to 0.76)	0.16	0.88 (−1.51 to 3.27)	0.25
Gender	0.13 (−0.03 to 0.29)	0.11	0.11 (−0.06 to 0.26)	0.21
BCVA (per letter)	−0.19 (−0.59 to −0.21)	<0.01	−0.28 (−3.38 to −1.61)	0.02
Baseline CRT (per 100um)	−0.82 (−1.22 to −0.42)	0.03	−0.98 (−1.56 to −0.40)	0.04
Total lesion area (mm ³)	−0.75 (−1.93 to 0.44)	0.21	−0.65 (−1.76 to 0.45)	0.59
BNN area(mm ³)	−1.18 (−2.83 to 0.46)	0.16	−0.92 (−2.47 to 0.63)	0.55
PL area (mm ³)	−0.67 (−3.83 to 2.49)	0.67	−0.90 (−3.84 to 2.04)	0.51
PED height (per 100um)	−1.04 (−3.60 to 1.52)	0.1	−0.73 (−2.08 to 0.62)	0.5
PED volume (nl)	−1.02 (−1.35 to −0.68)	<0.01	−0.09 (−0.19 to 0.10)	0.31
Subfoveal Choroidal Thickness (μm)	−0.76 (−2.79 to 1.26)	0.45	−0.47 (−30.54 to 29.59)	0.95
Choroidal volume (nl)	−1.66 (−3.59 to 0.26)	0.09	0.37 (−4.96 to 5.69)	0.48
Choroidal vascular hyperpermeability				
Absent	Ref		Ref	
Mild	−4.14 (−13.33 to 5.05)	0.37	−3.51 (−12.66 to 5.65)	0.45
Marked	−4.64 (−14.26 to 4.97)	0.33	−4.73 (−14.27 to 4.80)	0.32
Choroidal vascularity Index	−0.49 (−4.31 to 3.34)	0.78	2.72 (−20.51 to 25.96)	0.66
Number of injections received	2.56 (−2.24 to 7.37)	0.29	2.02 (−3.42 to 7.45)	0.62

Table 2. Linear regression analysis of baseline characteristics against BCVA change at month 12. *BNN* branching neovascular network, *PL* polypoidal lesion, *CRT* central retinal thickness, *PED* pigment epithelium detachment, *CVH* choroidal vascular hyper-permeability; *CVH* defined as marked = presence of patchy hyper fluorescence with blurred margins persisting from the mid to the late phase ICGA, mild = fuzziness of choroidal vessels in mid-phase ICGA but no patchy hyper fluorescence in late phase, absent = none of the above features present; *CV* choroidal volume; *CVI* choroidal vascularity index. Multivariate analysis adjusted for age and sex. Bold font denotes parameters significantly influencing the change in BCVA at month 12 from baseline and are retained in the final multivariable model.

Discussion

In this prospective clinical trial of aflibercept where participants were randomized to either fixed dosing or personalized treat and extend regimen, we identified that the baseline PED volume, PED height, CVH and CVI were significantly associated with disease activity at month 12.

Traditional quantitative metrics that are measured on SD-OCT pertaining to PEDs are its height and width although it is a three-dimensional focal elevation of the reflective RPE band over an optically clear or moderately reflective space and is one of the most distinct features of PCV²⁹. With recent advances in segmentation algorithms, volumetric analysis of retinal pathological features such as IRF, SRF and PED have been suggested as useful biomarkers for predicting treatment response³⁶. We measured the PED volume and included this parameter amongst the other traditionally acquired explanatory variables in the multiple regression model of disease activity which was the dependent variable. PED volume was retained in the final model, indicating that it contributes to explaining more of the variance in disease activity than PED height alone. The more accurate assessment of the PED as three-dimensional structure and the detection that a greater reduction in the PED volume was associated with better outcomes is therefore of clinical value and importance (Fig. 3).

Another key feature of PCV is the choroidal architecture. Dilated choroidal vessels and choroidal hyperpermeability have been hypothesized etiological processes that lead to PCV^{37,38}. A novel feature that we evaluated was the volumetric CVI. While some prior studies have evaluated CVI based on a single subfoveal B-scan OCT, the current study evaluated volumetric CVI across the 6 × 6 mm macular area³⁹. Our data suggest that a higher volumetric CVI is associated with active disease at month 12. The second choroidal feature we examined was CVH. We found that marked CVH was significantly associated with disease activity however neither an adverse nor beneficial association between CVH and visual outcome was noted at month 12. This is consistent with the equivocal results from studies that have assessed treatment outcomes and choroidal characteristics such as sub-foveal choroidal thickness and CVH^{40–44}. A recent study reported that the presence of CVH favorably influenced visual outcome with lower number of anti VEGF treatments combined with PDT¹⁴. However other studies have shown that the presence of CVH was associated with poor visual and anatomical outcomes after treatment with anti VEGF^{31,44}.

CVI and CVH may reflect the structural and functional alterations, respectively, in eyes with PCV and may be surrogate markers indicative of choroidal congestion. More severe alteration in these parameters as a cause or consequence of disease indicate a more extensive choroidal involvement with pathological alterations of choroidal vascular architecture and may hence be associated with poorer outcomes with treatment.

In addition to morphology at baseline, we also evaluated if the treatment response on completion of the loading phase influenced the visual and disease activity outcome at month 12. It was notable that a larger reduction in CRT and PED volume from baseline to month 3 was associated with better visual outcome and disease inactivity at month 12. Therefore, in addition to widely accepted markers of activity like SRF and IRF in typical nAMD, we postulate that PED volume is an important imaging biomarker that may help in the risk stratification

		Active (n = 13)	Inactive (n = 39)	OR (univariable)	p	OR (multi-variable)	p
Age	Mean (SD)	68.8 (8.2)	69.3 (8.9)	1.01 (0.94–1.09)	0.84	1.00 (0.80–1.21)	0.95
Gender, male	n (%)	8 (61.5)	25 (64.1)	0.90 (0.25–3.45)	1	0.93 (0.69–1.23)	0.87
Baseline lesion characteristics							
Total lesion area (mm ³)	Mean (SD)	4.2 (4.1)	4.0 (3.0)	0.98 (0.82–1.23)	0.85	0.90 (0.72–1.16)	0.36
BNN area (mm ³)	Mean (SD)	3.3 (3.4)	2.9 (1.9)	0.93 (0.72–1.23)	0.57	0.87 (0.63–1.20)	0.34
PL area (mm ³)	Mean (SD)	1.0 (1.0)	1.2 (1.3)	1.17 (0.70–2.65)	0.62	0.82 (0.45–1.23)	0.58
Baseline CRT (μm)	Mean (SD)	612.0 (188.0)	366.0 (129.5)	0.59 (0.32–0.88)	< 0.01	0.82 (0.69–0.90)	0.02
Baseline PED characteristics							
PED height (μm)	Mean (SD)	542.0 (298.0)	242.0 (150.0)	0.67 (0.53–0.88)	< 0.01	0.87 (0.63–0.94)	< 0.01
PED volume (nl)	Mean (SD)	2433 (1064)	799 (457)	0.94 (0.88–0.98)	< 0.01	0.77 (0.64–0.87)	0.02
Baseline Choroidal characteristics							
Choroidal vascular Hyperpermeability (CVH)							
Absent	n (%)	3 (23.1)	20 (51.2)	Ref		Ref	NA
Mild	n (%)	4 (30.8)	12 (23.1)	1.18 (0.76–2.34)	0.55	1.12 (0.80–2.23)	0.58
Marked	n (%)	6 (46.2)	7 (17.9)	1.65 (1.05–2.45)	0.03	1.69 (1.05–3.43)	0.04
Subfoveal Choroidal Thickness (μm)	Mean (SD)	289.0 (104.0)	258.0 (138.0)	0.83 (0.58–1.16)	0.31	0.80 (0.48–1.29)	0.37
Choroidal Volume (nl)	Mean (SD)	7772 (2044)	6293 (1837)	0.66 (0.44–0.93)	0.02	0.74 (0.32–1.42)	0.22
Choroidal vascularity Index (CVI)	Mean (SD)	63.0 (1.4)	61.8 (1.4)	0.81 (0.24–0.91)	0.02	0.78 (0.49–0.9)	0.04
Number of injections	Mean (SD)	8 (1.0)	8 (1.0)	0.89 (0.38–1.94)	0.8	0.83 (0.53–1.25)	0.08

Table 3. Linear regression analysis of baseline characteristics against disease activity status at month 12. *BNN* Branching neovascular network, *PL* polypoidal lesion, *CRT* central retinal thickness, *PED* pigment epithelium detachment, *CVH* choroidal vascular hyper-permeability; CVH defined as marked = presence of patchy hyper fluorescence with blurred margins persisting from the mid to the late phase ICGA, mild = fuzziness of choroidal vessels in mid-phase ICGA but no patchy hyper fluorescence in late phase, absent = none of the above features present, *CV* choroidal volume, *CVI* choroidal vascularity index. Multivariate analysis adjusted for age, sex and total number of injections. Bold fonts denote parameters significantly influencing the disease activity at month 12 from baseline and are retained in the final multivariable model.

in PCV. This is biologically plausible as sub-RPE fluid accumulation is a reflection of active polypoidal lesion(s) and/or the associated type-1 neovascular network.

The strengths of this study are its prospective collection of robust data, with morphology graded in the reading center by trained graders who were masked to clinical information and who used a pre-specified grading protocol. All the volumetric readouts were meticulously checked to ensure that SD-OCT segmentation was accurate as distortion of the RPE is common in eyes with PCV. Our study has a number of limitations. Our sample size was a moderate-sized cohort. The grading of CVH is subjective and can be affected by imaging technique. PED volume and CVI measurements were performed using non-commercially available software therefore have limited generalizability. One of the limitations of CVI measurement currently is the accuracy in defining the CSI. The choroidal segmentation can be challenging in eyes with thick choroids, especially in eyes with overlying retinal pathology which results in masking of CSI. In addition, there is currently no ideal binarization algorithm to determine the CVI especially in cases where the visualization of the choroid is affected by the overlying pathology. In this study, eyes with poor quality scans were excluded from CVI analysis. Each b scan included was assessed for segmentation accuracy and corrected manually if necessary.

In conclusion, the current analysis identified PCV-specific features that predict treatment outcomes and likely to be useful in guiding retreatment decisions. This preliminary data demonstrates the potential for PED-related volumetric parameters as an additional marker of disease activity however further studies are needed to establish its usefulness in retreatment decisions. With the increasing popularity of anti VEGF monotherapy in the treatment for PCV, these novel findings may improve treatment success in personalized retreatment regimens.

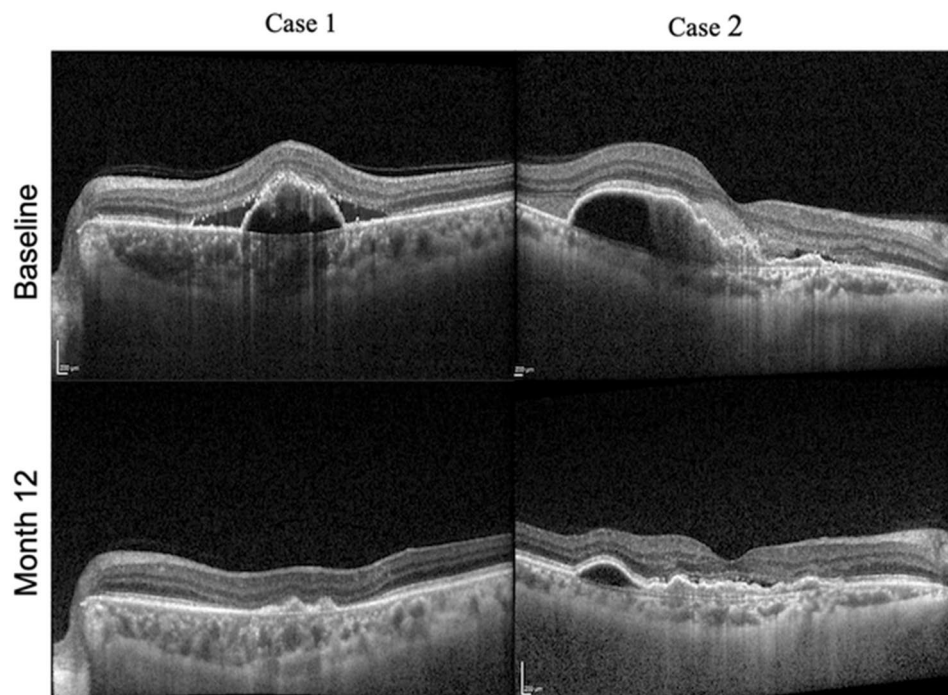


Figure 3. OCT images from 2 eyes showing the change in PED from baseline to month 12. Case 1: Baseline OCT scan showing a large PED with subretinal fluid constituting most of the CRT (367 μm) with PED volume of 0.81 nl and maximum PED height of 338 μm . Month 12 OCT scan showing resolution of PED and subretinal fluid with reduction in CRT (165 μm), PED height (67 μm) and PED volume (0.1 nl). Case 2: Baseline OCT scan showing a large sub-foveal PED with SRHM occupying most of the CRT (446 μm) with PED volume of 2.1 nl and maximum PED height of 362 μm . Month 12 OCT scan showing reduction in CRT (220 μm), PED height (171 μm) and PED volume (0.88 nl) along with resolution of SRHM.

Response feature	Univariate beta	<i>p</i>	Multivariate beta	<i>p</i>
Association with gain in BCVA in letters				
Baseline to month 3 mean change in CRT (per 100 nm)	1.67 (0.45 to 2.90)	0.02	0.51 (0.12 to 2.18)	0.03
Baseline to month 3 mean change in PED volume (per 100 nl)	0.93 (0.20 to 1.66)	0.01	1.04 (0.07 to 2.01)	0.03
Baseline to month 3 mean change in PED height (per 100um)	0.01 (-0.01 to 0.03)	0.25	-0.00 (-0.03 to 0.02)	0.78
Baseline to month 3 mean change in CV (per 100 nl)	-0.01 (-1.28 to 1.25)	0.98	0.22 (-0.96 to 1.40)	0.71
Association with inactive disease				
Baseline to month 3 mean change in CRT (per 100 nm)	1.72 (1.16 to 2.80)	0.01	1.32 (1.03 to 2.82)	0.03
Baseline to month 3 mean change in PED volume (per 100 nl)	1.42 (1.18 to 1.79)	0.01	1.39 (1.11 to 1.82)	0.01
Baseline to month 3 mean change in PED height (per 100um)	0.91 (0.49 to 1.15)	0.62	1.00 (0.44 to 1.30)	0.98
Baseline to month 3 mean change in CV(per 100 nl)	1.42 (1.05 to 2.03)	0.03	0.83 (0.44 to 1.48)	0.56

Table 4. Association of treatment outcomes at month 3 with outcomes at month 12. CRT central retinal thickness, PED pigment epithelium detachment, CV choroidal volume; Multivariate analysis adjusted for age, sex and number of injections. Bold fonts denotes parameters significantly influencing the gain in BCVA and disease activity at month 12 from baseline and are retained in the final multivariable model.

Received: 13 June 2021; Accepted: 27 January 2022

Published online: 22 February 2022

References

- Busbee, B. G., Ho, A. C. & Brown, D. M. *et al.* Twelve-month efficacy and safety of 0.5 mg or 2.0 mg ranibizumab in patients with subfoveal neovascular age-related macular degeneration. *Ophthalmology* **2013**,**120**:1046–56. <https://doi.org/10.1016/j.ophtha.2012.10.014>
- Wykoff, C. C. *et al.* Prospective trial of treat-and-extend versus monthly dosing for neovascular age-related macular degeneration: TREX-AMD 1-year results. *Ophthalmology* **122**, 2514–2522. <https://doi.org/10.1016/j.ophtha.2015.08.009> (2015).
- Ying, G. *et al.* Association of baseline characteristics and early vision response with 2-year vision outcomes in the comparison of AMD treatments trials (CATT). *Ophthalmology* **122**, 2523–2531.e1. <https://doi.org/10.1016/j.ophtha.2015.08.015> (2015).
- Yannuzzi, L. A. *et al.* Polypoidal choroidal vasculopathy and neovascularized age-related macular degeneration. *Arch. Ophthalmol.* **117**, 1503–1510. <https://doi.org/10.1001/archophth.117.11.1503> (1999).
- Lafaut, B. A. *et al.* Polypoidal choroidal vasculopathy in Caucasians. *Graefes Arch. Clin. Exp. Ophthalmol.* **238**, 752–759. <https://doi.org/10.1007/s004170000180> (2000).
- Wong, C. W., Wong, T. Y. & Cheung, C. M. G. Polypoidal choroidal vasculopathy in Asians. *J. Clin. Med.* **4**, 782–821. <https://doi.org/10.3390/jcm4050782> (2015).
- Balaratnasingam, C. *et al.* Polypoidal choroidal vasculopathy: A distinct disease or manifestation of many?. *Retina* **36**, 1–8. <https://doi.org/10.1097/IAE.0000000000000774> (2016).
- Cheung, C. M. G. *et al.* Polypoidal choroidal vasculopathy: Definition, pathogenesis, diagnosis, and management. *Ophthalmology* **125**, 708–724. <https://doi.org/10.1016/j.ophtha.2017.11.019> (2018).
- Chong Teo, K. Y. *et al.* A multicountry comparison of real-world management and outcomes of polypoidal choroidal vasculopathy: Fight retinal blindness! Cohort. *Ophthalmol. Retina* **3**, 220–229. <https://doi.org/10.1016/j.oret.2018.11.003> (2019).
- Teo, K. Y. C., Gillies, M. & Fraser-Bell, S. The use of vascular endothelial growth factor inhibitors and complementary treatment options in polypoidal choroidal vasculopathy: A subtype of neovascular age-related macular degeneration. *Int. J. Mol. Sci.* **2018**. <https://doi.org/10.3390/ijms19092611>
- Hjji, M. *et al.* Efficacy and safety of intravitreal aflibercept treat-and-extend regimens in exudative age-related macular degeneration: 52- and 96-week findings from ALTAIR: A randomized controlled trial. *Adv. Ther.* **37**, 1173–1187. <https://doi.org/10.1007/s12325-020-01236-x> (2020).
- Wong, T. Y. *et al.* Efficacy and safety of intravitreal aflibercept for polypoidal choroidal vasculopathy: Two-year results of the aflibercept in polypoidal choroidal vasculopathy study. *Am. J. Ophthalmol.* **204**, 80–89. <https://doi.org/10.1016/j.ajo.2019.02.027> (2019).
- Hirakata, T. *et al.* One-year outcome of intravitreal aflibercept injection for age-related macular degeneration resistant to ranibizumab: Rapid morphologic recovery and subsequent visual improvement. *Clin. Ophthalmol.* **10**, 969–977. <https://doi.org/10.2147/OPHTH.S101596> (2016).
- Yanagi, Y. *et al.* Choroidal vascular hyperpermeability as a predictor of treatment response for polypoidal choroidal vasculopathy. *Retina* **38**, 1509–1517. <https://doi.org/10.1097/IAE.0000000000001758> (2018).
- Teo, K. Y. C. *et al.* Comparison of optical coherence tomography angiographic changes after anti-vascular endothelial growth factor therapy alone or in combination with photodynamic therapy in polypoidal choroidal vasculopathy. *Retina* **38**, 1675–1687. <https://doi.org/10.1097/IAE.0000000000001776> (2018).
- Cho, H. J. *et al.* Effects of choroidal vascular hyperpermeability on anti-vascular endothelial growth factor treatment for polypoidal choroidal vasculopathy. *Am. J. Ophthalmol.* **156**, 1192–1200.e1. <https://doi.org/10.1016/j.ajo.2013.07.001> (2013).
- Nomura, Y. & Yanagi, Y. Intravitreal aflibercept for ranibizumab-resistant exudative age-related macular degeneration with choroidal vascular hyperpermeability. *Jpn. J. Ophthalmol.* **59**, 261–265. <https://doi.org/10.1007/s10384-015-0387-z> (2015).
- Kang, H. M. *et al.* Subfoveal choroidal thickness as a potential predictor of visual outcome and treatment response after intravitreal ranibizumab injections for typical exudative age-related macular degeneration. *Am. J. Ophthalmol.* **157**, 1013–1021. <https://doi.org/10.1016/j.ajo.2014.01.019> (2014).
- Kim, H. *et al.* Subfoveal choroidal thickness as a predictor of treatment response to anti-vascular endothelial growth factor therapy for polypoidal choroidal vasculopathy. *Graefes Arch. Clin. Exp. Ophthalmol.* **254**, 1497–1503. <https://doi.org/10.1007/s00417-015-3221-x> (2016).
- Jirattanasopa, P. *et al.* Choroidal thickness, vascular hyperpermeability, and complement factor H in age-related macular degeneration and polypoidal choroidal vasculopathy. *Investig. Ophthalmol. Vis. Sci.* **53**, 3663–3672. <https://doi.org/10.1167/iovs.12-9619> (2012).
- Cheung, C. M. G. *et al.* The evolution of fibrosis and atrophy and their relationship with visual outcomes in asian persons with neovascular age-related macular degeneration. *Ophthalmol. Retina* **3**, 1045–1055. <https://doi.org/10.1016/j.oret.2019.06.002> (2019).
- Chan, E. W. *et al.* Quantitative changes in pigment epithelial detachment area and volume predict retreatment in polypoidal choroidal vasculopathy. *Am. J. Ophthalmol.* **177**, 195–205. <https://doi.org/10.1016/j.ajo.2016.12.008> (2017).
- Freeman, W. R. *et al.* Prognostic implications of pigment epithelial detachment in bevacizumab (avastin)-treated eyes with age-related macular degeneration and choroidal neovascularization. *Retina* **31**, 1812–1818. <https://doi.org/10.1097/IAE.0b013e31821987a4> (2011).
- Khanani, A. M. *et al.* Optimal management of pigment epithelial detachments in eyes with neovascular age-related macular degeneration. *Retina* **38**, 2103–2117. <https://doi.org/10.1097/IAE.0000000000002195> (2018).
- Balaskas, K. *et al.* Quantitative analysis of pigment epithelial detachment response to different anti-vascular endothelial growth factor agents in wet age-related macular degeneration. *Retina* **37**, 1297–1304. <https://doi.org/10.1097/IAE.0000000000001342> (2017).
- Sarraf, D. *et al.* Ranibizumab treatment for pigment epithelial detachment secondary to neovascular age-related macular degeneration: post hoc analysis of the HARBOR Study. *Ophthalmology* **123**, 2213–2224. <https://doi.org/10.1016/j.ophtha.2016.07.007> (2016).
- Waldstein, S. M. *et al.* Predictive value of retinal morphology for visual acuity outcomes of different ranibizumab treatment regimens for neovascular AMD. *Ophthalmology* **123**, 60–69. <https://doi.org/10.1016/j.ophtha.2015.09.013> (2016).
- Tyagi, P. *et al.* Clinical response of pigment epithelial detachment associated with neovascular age-related macular degeneration in switching treatment from Ranibizumab to Aflibercept. *BMC Ophthalmol.* **18**, 148. <https://doi.org/10.1186/s12886-018-0824-0> (2018).
- Broadhead, G. K. *et al.* Response of pigment epithelial detachments to intravitreal aflibercept among patients with treatment-resistant neovascular age-related macular degeneration. *Retina* **35**, 975–981. <https://doi.org/10.1097/IAE.0000000000000409> (2015).
- Chhablani, J. *et al.* Repeatability and reproducibility of manual choroidal volume measurements using enhanced depth imaging optical coherence tomography. *Investig. Ophthalmol. Vis. Sci.* **53**, 2274–2280. <https://doi.org/10.1167/iovs.12-9435> (2012).
- Sonoda, S. *et al.* Responsiveness of eyes with polypoidal choroidal vasculopathy with choroidal hyperpermeability to intravitreal ranibizumab. *BMC Ophthalmol.* **13**, 43. <https://doi.org/10.1186/1471-2415-13-43> (2013).

32. Wei, X. *et al.* Choroidal Vascularity Index: A novel optical coherence tomography based parameter in patients with exudative age-related macular degeneration. *Retina* **37**, 1120–1125. <https://doi.org/10.1097/IAE.0000000000001312> (2017).
33. Ting, D. S. W. *et al.* Choroidal remodeling in age-related macular degeneration and polypoidal choroidal vasculopathy: A 12-month prospective study. *Sci. Rep.* **7**, 7868. <https://doi.org/10.1038/s41598-017-08276-4> (2017).
34. Teo, K. Y. C., Jordan-Yu, J. M. & Tan, A. C. S. *et al.* Efficacy of a novel personalised aflibercept monotherapy regimen based on polypoidal lesion closure in participants with polypoidal choroidal vasculopathy. *Br J Ophthalmol.* <https://doi.org/10.1136/bjophthalmol-2020-318354>
35. Tan, C. S. *et al.* EVEREST study report 2: Imaging and grading protocol, and baseline characteristics of a randomised controlled trial of polypoidal choroidal vasculopathy. *Br. J. Ophthalmol.* **99**, 624–628. <https://doi.org/10.1136/bjophthalmol-2014-305674> (2015).
36. Keenan, T. D. L. *et al.* Automated quantitative assessment of retinal fluid volumes as important biomarkers in neovascular age-related macular degeneration. *Am. J. Ophthalmol.* **224**, 267–281. <https://doi.org/10.1016/j.ajo.2020.12.012> (2021).
37. Sasahara, M. *et al.* Polypoidal choroidal vasculopathy with choroidal vascular hyperpermeability. *Am. J. Ophthalmol.* **142**, 601–607. <https://doi.org/10.1016/j.ajo.2006.05.051> (2006).
38. Chung, S. E. *et al.* Choroidal thickness in polypoidal choroidal vasculopathy and exudative age-related macular degeneration. *Ophthalmology* **118**, 840–845. <https://doi.org/10.1016/j.ophtha.2010.09.012> (2011).
39. Agrawal, R., Gupta, P. & Tan, K. A. *et al.* Choroidal vascularity index as a measure of vascular status of the choroid: Measurements in healthy eyes from a population-based study. *Sci. Rep.* 2016. <https://doi.org/10.1038/srep21090>
40. Cho, H. J. *et al.* Response of pigment epithelial detachment to anti-vascular endothelial growth factor treatment in age-related macular degeneration. *Am. J. Ophthalmol.* **166**, 112–119. <https://doi.org/10.1016/j.ajo.2016.03.039> (2016).
41. Yamashita, M. *et al.* Response of serous retinal pigment epithelial detachments to intravitreal aflibercept in polypoidal choroidal vasculopathy refractory to ranibizumab. *Clin. Ophthalmol.* **8**, 343–346. <https://doi.org/10.2147/OPTH.S56539> (2014).
42. Hata, M. *et al.* Efficacy of intravitreal injection of aflibercept in neovascular age-related macular degeneration with or without choroidal vascular hyperpermeability. *Investig. Ophthalmol. Vis. Sci.* **55**, 7874–7880. <https://doi.org/10.1167/iovs.14-14610> (2014).
43. Koizumi, H. *et al.* Subfoveal choroidal thickness in typical age-related macular degeneration and polypoidal choroidal vasculopathy. *Graefes Arch. Clin. Exp. Ophthalmol.* **249**, 1123–1128. <https://doi.org/10.1007/s00417-011-1620-1> (2011).
44. Koizumi, H. *et al.* Relationship between clinical characteristics of polypoidal choroidal vasculopathy and choroidal vascular hyperpermeability. *Am. J. Ophthalmol.* **155**, 305–313.e1. <https://doi.org/10.1016/j.ajo.2012.07.018> (2013).

Author contributions

K.T., J.J., C.H.V. and G.C. developed the study design, conducted the analysis and prepared the manuscript and figures; K.T., A.T., B.F., S.S. and G.C. recruited patients. J.J., C.H.V., H.S., M.A. and K.T. graded the images and K.T. performed the statistical analysis. G.C., U.C. were the senior authors who edited and reviewed the manuscript and provided the scientific expert advice on the manuscript.

Funding

This study is supported by the National Medical Research Council Open Fund Large Collaborative grant: NMRC/LGC/004/2018. The funding organization had no role in the design or conduct of this research.

Competing interests

The authors declare no competing interests.

Additional information

Correspondence and requests for materials should be addressed to K.Y.C.T.

Reprints and permissions information is available at www.nature.com/reprints.

Publisher's note Springer Nature remains neutral with regard to jurisdictional claims in published maps and institutional affiliations.



Open Access This article is licensed under a Creative Commons Attribution 4.0 International License, which permits use, sharing, adaptation, distribution and reproduction in any medium or format, as long as you give appropriate credit to the original author(s) and the source, provide a link to the Creative Commons licence, and indicate if changes were made. The images or other third party material in this article are included in the article's Creative Commons licence, unless indicated otherwise in a credit line to the material. If material is not included in the article's Creative Commons licence and your intended use is not permitted by statutory regulation or exceeds the permitted use, you will need to obtain permission directly from the copyright holder. To view a copy of this licence, visit <http://creativecommons.org/licenses/by/4.0/>.

© The Author(s) 2022